ACS OMEGA

Cite This: ACS Omega XXXX, XXX, XXX−XXX

Article

http://pubs.acs.org/journal/acsodf

Photo-Assisted Removal of Tetracycline Using Bio-Nanocomposite-Immobilized Alginate Beads

Geetha Gopal, Namrata Roy, Natarajan Chandrasekaran, and Amitava Mukherjee*

Centre for NanoBiotechnology, VIT, Vellore 632014, Tamil Nadu, India

Supporting Information

ABSTRACT: In the present study, we report an efficient method for tetracycline (TC) removal from contaminated wastewater using alginate beads, immobilized with bio nanocomposite (BNC) consisting of Fe_3O_4 (iron oxide) and TiO_2 (titanium dioxide) nanoparticles along with dead biomass of TC-resistant bacteria *Acinetobacter* sp. Chemically synthesized Fe_3O_4 nanoparticles and commercially available TiO_2 (P_{25}) nanoparticles were combined to form nanocomposite followed by encapsulation within alginate beads along with heat-killed biomass of *Acinetobacter*sp. for the efficient degradation and adsorption of the target pollutant. The primary characterization of chemically synthesized nanoparticles was carried out with Fourier transform infrared, scanning electron microscopy−energy-dispersive X-ray spectrometry, transmission electron microscopy, and X-ray diffraction techniques. The batch studies for TC removal were performed by varying the reaction parameters such as bead weight, initial TC concentration, and pH in a photoreactor with UV-C irradiation. TC concentration of 10 mg/L, bead weight 10 g, and pH 6 were fixed as the optimum condition where 98 ± 0.5% of TC was removed from the solution. The possible removal mechanism was investigated with the help of UV−visible, total organic carbon, oxidation−reduction potential, Brunauer−Emmett−Teller, and liquid chromatography−mass spectroscopy analyses. The applicability of the process was successfully tested with the natural water systems spiked with TC at 10 mg/L. To assess the ecotoxic effects of the treated effluents, the cell viability assay was performed with the algal strains, *Chlorella*, and *Scenedesmus*sp. and the bacterial strains, *Pseudomonas aeruginosa*and *Escherichia coli*. Finally, the reusability of the BNC bead was successfully established up to the 4th cycle.

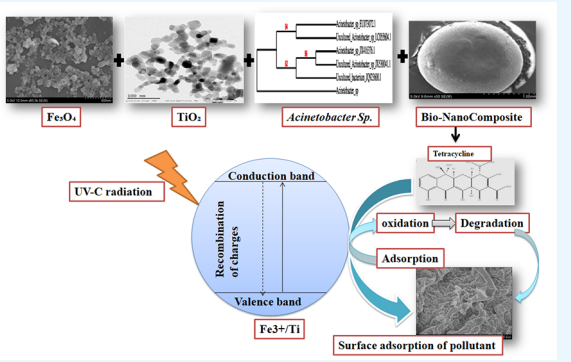

1. INTRODUCTION

Widespread usage of antibiotics in human and veterinary applications has made natural water system rife with organic pollutants.[1] The very first reported water contamination due to antibiotic pollutants was reported in England by Watts et al.[2] They identified a mixture of antibiotics like tetracycline (TC), macrolides, and sulphonamides in natural water system up to the concentration of 1 mg/L way higher than the permissible limit.[2] Minimal cost and ease of large-scale production favors the wide use of TC in agricultural, human, and veterinary applications.[3] TC administration in humans and animals, in turn, results in about 90% of its release into the environment, especially the natural water systems in the active form.[4] The presence of TC in the natural water system brings in toxic effects to aquatic and human life and may lead to antibiotic resistance in bacteria.[5]

Conventional methods of wastewater treatment make use of membrane filtration, chemical reactors (photochemical, electrochemical, advanced oxidation, ozonation, and photocatalytic process), and adsorbents for the removal of various organic pollutants. Among these, the adsorption-based antibiotic removal is profitable as it makes use of a simple separation technique, cost-effective, easy to perform, and less toxic to the environment.[6,7]

Adsorption of contaminants only involves the transformation of antibiotics from one phase to another without any degradation. Hence, a suitable method is required for degrading the contaminants into less harmful byproducts.[9] A recent method, the advanced oxidation process (AOP) involves the formation of hydroxyl radicals which converts such antibiotics into harmless products under UV irradiation with various nanoparticles like ZnO, TiO_2, and H_2O_2.[10]

Nanoparticles are suitable for the oxidation process because of their high photocatalytic activity, relatively stable in aqueous solution, nontoxic nature, and low cost.[11] It was reported that TiO_2/UV-A-based photocatalytic degradation followed by adsorption of pharmaceutical compounds is more advantageous over the conventional antibiotic removal techniques,[12] as it involves fast mineralization and detoxification of the antibiotic by photocatalytic ozonation.[13] However, in spite of its advantages, TiO_2-based antibiotic removal has reduced

Received: July 25, 2019
Accepted: September 19, 2019

DOI: 10.1021/acsomega.9b02339
ACS Omega XXXX, XXX, XXX−XXX

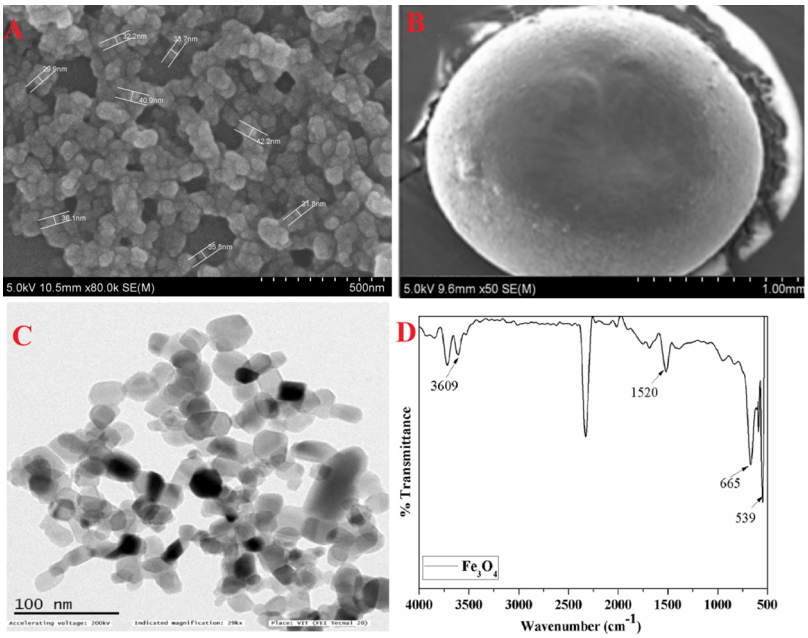

Figure 1. (A) SEM image of iron oxide nanoparticle, (B) SEM image of the BNC bead, (C) TEM image of procured TiO_2 (P_{25}) nanoparticle, (D) FT-IR spectrum of the Fe_3O_4 nanoparticle.

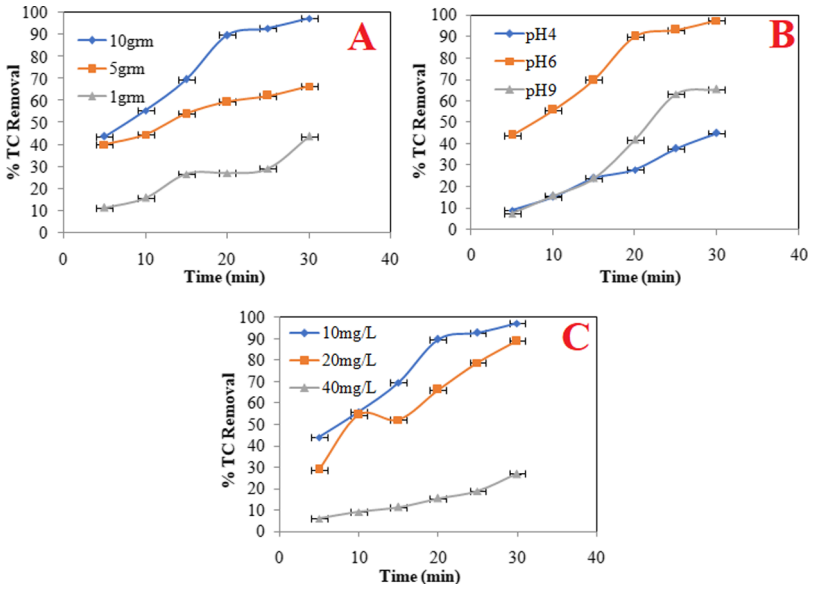

Figure 2. Determination of TC removal percentage by (A) effect of bead weight 1, 5 and 10 g loaded with BNC, (B) effect of pH 4, 6 and 9, (C) effect of initial TC concentration 10, 20, and 40 mg/L.

photocatalytic effect because of the formation of electron−hole recombination; hence, to prevent this effect, Ti can be fortified with other metals especially with Fe^{3+}. TiO_2 was effectively doped with Fe^{3+} because of its half-full electron configuration and relatively equal ionic radius with Ti nanoparticles.[14]

Fe^{3+}−TiO_2/UV-C based photocatalytic degradation removed 88.92% of amoxicillin from wastewater but it required pretreatment methods for the enhanced removal in natural water samples[11] and the nanophotocatalyst, Fe^{3+}−TiO_2 with UV-C radiation was used to remove up to 97% of metronidazole from the aqueous system.[15] Also, the occurrence of penicillin-G was reduced to more than 90% with Fe^{3+}−TiO_2/UV-A photocatalytic treatment and this technique was reported as the most efficient and cost-effective method for the removal of the penicillin.[14]

Wastewater treatment technique based on adsorption also relies on biosorbents like bacteria, fungi, algae, yeasts, and agricultural waste. The main attributes of biosorption include rapid adsorption rate, high selectivity and efficiency, and cost-effectiveness. Hence, this method can be used as an efficient alternative to the existing carbon-based adsorption techniques.[16] β-Lactam antibiotics like penicillin-G were effectively adsorbed by dried *Rhizopus arrhizus* and activated sludge. This material can be used as an alternative for carbon nanomaterials because of its low cost and increased selectivity toward antibiotics.[17]

DOI: 10.1021/acsomega.9b02339
ACS Omega XXXX, XXX, XXX−XXX

Table 1. Comparison of TC Degradation Efficiency with Different Photocatalyst

photocatalyst	reaction condition	% TC removal	ref
UV/TiO_2/H_2O_2	catalyst conc. 1.0 g/L of TiO_2, 100 mg/L of H_2O_2, TC conc. 55 mg/L, pH 5	100	Safari et al.[10]
UV/MIL-101(Fe)/TiO_2	catalyst conc. 0.6 g/L, TC conc. 20 mg/L, pH 7	95.95	He et al.[27]
UV/TiO_2	catalyst conc. 0.5 g/L, TC conc. 40 mg/L, pH 6.0	100	Reyes et al.[28]
UV/TiO-rGO-AC	catalyst conc. 0.8 g/L, TC conc. 40 mg/L	70	Qu et al.[29]
Cu_2O−TiO_2-Pal	catalyst conc. 1 g/L, TC conc. 30 mg/L, pH 8.7	88.81	Shi et al.[30]
UV/BNC bead	catalyst conc. 2:2:1 (TiO_2/Fe_3O_4/dead biomass) bead weight: 10 g, pH 6.0, TC conc. 10 mg/L	98.61	present work

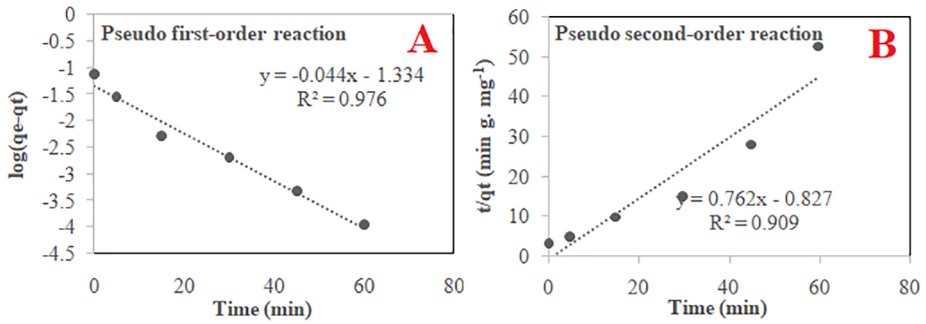

Figure 3. Kinetic study of TC removal by BNC with UV-C radiation (A) pseudo-first-order kinetic model with k_1 = 0.044 and R_1 = 0.976 (B) pseudo second-order kinetic model with k_2 = 0.762 and R_2 = 0.909.

In the current study, we used the dead biomass of *Acinetobacter*sp. isolated from the TC-contaminated site. Even though, there are several studies regarding the removal of antibiotics by AOP, we did not find any specific report on coupling distinct advantages of antibiotic-resistant bacterial biomass with photocatalytic potential of nanomaterials to degrade the antibiotics. Herein, we report a novel nanobiomaterial, that is, the fortified titanium dioxide (TiO_2) (P_{25}) catalyst with iron oxide NP and dead biomass immobilized over biodegradable polymer sodium alginate with UV-C irradiation for TC removal from aqueous solution. Bionanocomposite (BNC) preparation involves (a) the synthesis of iron oxide by chemical precipitation, (b) followed by the preparation of nanocomposite with synthetic TiO_2 (P_{25}), and finally combining with the dead biomass of *Acinetobacter* sp. which has high selectivity toward TC antibiotic. The prepared BNC was characterized and validated for the removal of TC from the natural water system.

2. RESULTS AND DISCUSSION

2.1. Characterization Studies. Figure 1A shows the scanning electron microscopy (SEM) image of the synthesized iron oxide nanoparticle, where the average size of the iron oxide nanoparticle was found in the range of 75−85 nm with a spherical structure. The surface morphology of the BNC beads was found to be smooth and uniform before interaction with TC and the average size of the bead was 500−600 μm (Figure 1B). Energy-dispersive X-ray spectrometry (EDX) analysis of the BNC bead showed the presence of the Fe, Ti content with 1.60 and 1.35 wt %, respectively (Table S2 Supporting Information). The transmission electron microscopy (TEM) image of the procured TiO_2 nanoparticle shows the particle diameter ranging from 50 to 200 nm with irregular shape[19] (Figure 1C).

The Fourier transform infrared (FT-IR) spectrum (Figure 1D) of Fe_3O_4 shows two intense peaks at 539 and 665 cm^{-1} corresponding to Fe−O stretching vibration[20] and the peak at 3609 cm^{-1} is assigned to OH bending and 1520 cm^{-1} corresponds to C=C aromatic vibration.[21]

2.2. Batch Removal of TC. *2.2.1. Effect of Bead Weight.* The BNC beads of different weight percentages (1, 5, and 10 g) were tested with 10 mg/L of TC solution. The anticipated increase in the amount of bead weight enhances the removal efficiency. Therefore, the TC removal increased to 98.61% by the application of 10 g of BNC beads at 30 min. The reduced dosage of the beads to that of the TC produced a lower removal efficiency of 33.72 and 66.46% for 1 and 5 g, respectively (Figure 2A). This indicates that the increase of the bead weight is proportionate with an increase in the efficiency of the TC removal.

2.2.2. Effect of pH. The tests were performed by varying the pH at 4, 6, and 9 with 10 g of the BNC bead and 10 mg/L of TC. The data showed that at pH 9 the percentage of removal was 40.2 ± 2.19 and at pH 4 51.34 ± 1.97, whereas at pH 6 optimal TC removal of 98.61 ± 1.07 was noted (Figure 2B).

2.2.3. Effect of Initial TC Concentration. Further tests were performed with increasing concentrations of TC from 10 to 40 mg/L. This condition leads to a decrease in the removal efficiency of the TC (Figure 2C). The highest removal efficiency of 98.61 ± 1.07% was obtained at 10 mg/L, whereas for 20 and 40 mg/L the removal percentage declined to 88.92 ± 1.04 and 48.93 ± 1.09, respectively, showing a reduction in removal efficiency by increasing TC concentration.

TC removal efficiency in the current study is compared with similar studies from literature in Table 1. The control study to determine the effect of individual nanoparticle and the dead biomass was performed under the optimum experimental conditions. The experimental data shows 12.74, 15.9, 16.63, and 19.12% of TC removal by alginate beads without loading, beads loaded with dead biomass, beads with Fe_3O_4 alone, and beads with TiO_2 nanoparticle alone, respectively (Figure S1 Supporting Information). To find out the effect of nonphoto-assisted removal, the control experiments were performed without any irradiation keeping the remaining conditions same

DOI: 10.1021/acsomega.9b02339
ACS Omega XXXX, XXX, XXX−XXX

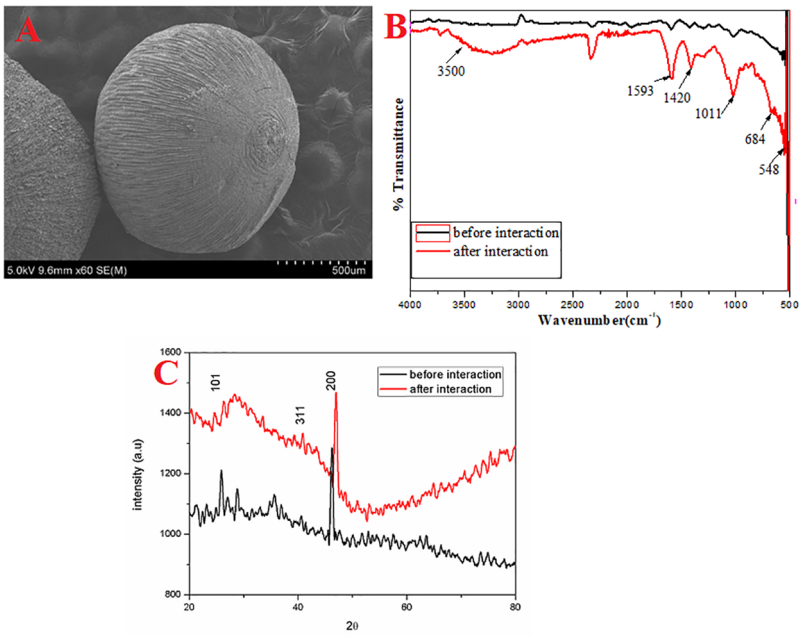

Figure 4. (A) SEM image of the alginate bead loaded with BNC before and after interaction (B) XRD analysis of the BNC bead before and after interaction with TC (C) FTIR spectrum of before and BNC bead before and after interaction with TC.

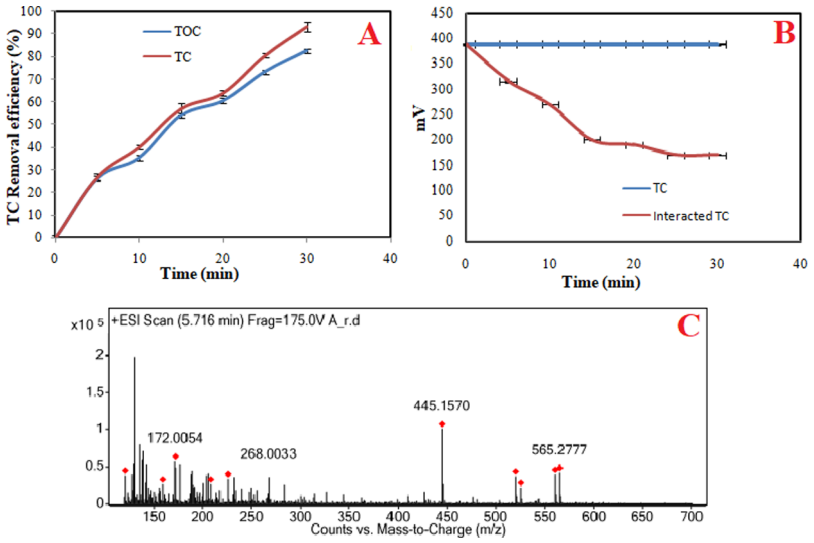

Figure 5. (A) % TC removal analysis by the TOC study (B) ORP measurement (C) HR-LC−MS analysis of the BNC bead-treated TC sample.

and only 16.16% of TC removal was obtained (Figure S2 Supporting Information).

2.3. Kinetics of TC Removal. The results from the kinetic study clearly showed that the mechanism followed the pseudo first-order kinetics with the regression value of approximately around 0.976 (Figure 3). The study suggests that the adsorption of the TC involves initial degradation followed by adsorption on alginate beads.[22]

2.4. TC Removal Mechanism. The SEM analysis (Figure 4A) of the BNC bead after the interaction showed rough surface morphology. It can be deduced that because of the adsorption of TC onto the surface of beads there is a change in surface morphology from smooth to rough.[23]

The X-ray diffraction (XRD) analysis of the BNC bead before interaction showed intense peaks at (101) and (200) corresponding to the anatase TiO_2 nanoparticle,[24] and the peak at (300) denoting the highly pure magnetite Fe formation[21] (Figure 4B). After the interaction with TC, the intensity of the crystalline phase of both TiO_2 and Fe−O reduced, which may be attributed to the degradation of antibiotics by the nanoparticle.

The FT-IR data, after interaction, showed slight shift of peaks observed at 2310.72, 651, and, 551 cm^{-1}. This can be due to adsorption of photocatalytically degraded TC through binding with the nanoparticles in the composite, through the formation of C−C, C−OH, and C−H rings[23] (Figure 4C). The possible surface adsorption of the antibiotic onto the BNC beads was further confirmed by surface area and porosity analysis of the beads before and after the interaction. From the analysis, it was noted that before interaction the surface area was 1.51 m^2/g and after interaction, it reduced to 0.27 m^2/g which confirmed that because of surface adsorption the porosity of the BNC beads decreased.

DOI: 10.1021/acsomega.9b02339
ACS Omega XXXX, XXX, XXX−XXX

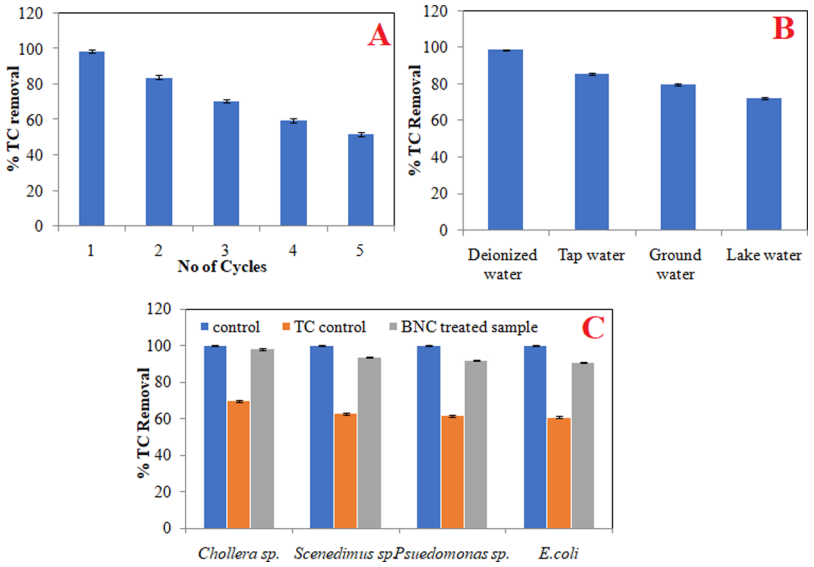

Figure 6. (A) Reusability assessment of BNC bead (B) effect of the BNC bead on natural water system (C) residual toxicity study of TC and BNC-treated TC sample against algal and bacterial strains.

The TC removal mechanism with respect to total organic carbon (TOC) content in the sample is displayed in Figure 5A, which shows steady decrease in TOC content along with decline in TC concentration. Absence of any degradation and adsorption of TC throughout the control test was confirmed because the TOC remained constant.[25] However, after the interaction the TOC content showed significant reduction proving notable role played by adsorption during the reaction. The maximum drop of TOC data was noted at 30 min corresponding to 98.61% removal.

To understand the role of a reducing agent in the degradation of antibiotic oxidation−reduction potential (ORP) analysis was performed and the data are shown in Figure 5B. The ORP value at time t_0 was 380 mV and at time t_{30} had ORP value reduced to 170 mV indicating the presence of strong reducing environment during the interaction.

The liquid chromatography−mass spectroscopy (LC−MS) analysis of the reacted liquid sample in Figure 5C shows that the intensity of the initial TC peak at 445 was reduced after 30 min of interaction with the BNC bead. The formation of intermediate byproducts was confirmed by the presence of peak at 172 and the peak at 130, which involves various structural and functional group modifications such as epimerization, dehydration, and dimethylation. The degraded byproducts can be easily adsorbed over the beads after interaction.[26]

2.5. Reusability of BNC. The reusability test in Figure 6A showed that BNC beads used in the experiment were viable until 4 cycles for the better removal of TC. Further, the stability of BNC beads and control beads under UV irradiation was analyzed for the deformities and it established stability of beads after continuous cycle of TC removal. The removal efficiency of control beads decreased after the 4th cycle with 4.8 ± 0.5% and for BNC beads 59 ± 0.5% of TC removal. This decrease in the adsorption capacity is probably due to binding of the TC-degraded products onto the nanoparticles present within the matrix of the BNC beads or because of the escape of the nanoparticles from the agile surface of the BNC beads. No deformation of the beads could be noted even after four cycles of interactions.

2.6. BNC for Real Water Sample Treatment. The effect of BNC bead on the natural water system adulterated with TC shows was 85.16 ± 0.4% of TC removal in tap water followed by groundwater with 79.62 ± 1.6% removal and lake water of 71.90 ± 0.2% removal Figure 6B. The percentage TC removal was reduced for the natural water system because of the presence of colloidal particles that are present in the water sources. Hence, it requires that the natural water system be pretreated before the application of the BNC bead for the most effective removal of TC.

2.7. Residual Toxicity of BNC. The toxicity assessment in Figure 6C showed that the percent cell viability of the two strains of algal species in the range of 98.075 ± 0.1 and 93.644 ± 0.2 for *Chlorella* and *Scenedesmus* sp. which states that the *Scenedesmus obliquus* is more sensitive to the BNC-treated TC sample compared to the *Chlorella* and which shows the percent cell viability of 69.79 ± 0.2 and 62.74 ± 0.3 against TC control. As for the bacterial strains of *Pseudomonas aeruginosa* and *E. coli,* the toxicity assessment was performed, which shows the percent cell viability of 91.83 ± 0.2 and 90.67 ± 0.1 for treated TC sample and 61.53 ± 0.2 and 60.75 ± 0.2 for TC control.

3. CONCLUSIONS

Application of the BNC-loaded alginate bead for the TC removal from the natural water system was proven with the removal percentage of 71.09 ± 0.2 which further increased by pretreatment of the real water sample to remove colloidal impurities. It was found that BNC-loaded alginate bead-based photocatalytic removal of TC will release considerably less toxic byproducts with increased reusability range and it can be easily separated out after the process. Hence, this method can be further modified for the removal of mixture of antibiotics with less cost and higher efficiency.

4. MATERIALS AND METHODS

4.1. Materials. TC ($C_{22}H_{24}N_2O_8$), ferric chloride ($FeCl_3$), and titanium dioxide (TiO_2) (P_{25}) were procured from Sigma-Aldrich, India and sodium borohydride ($NaBH_4$) was procured from HiMedia. The glassware used was of high-quality

DOI: 10.1021/acsomega.9b02339
ACS Omega XXXX, XXX, XXX−XXX

borosilicate glass and all other chemicals were of analytical grade. The bacterial strain *Acinetobacter* sp. was isolated from the contaminated site and confirmed by 16s rRNA sequencing.

4.2. Synthesis of Iron Oxide Nanoparticles. Synthesis of iron oxide nanoparticles by co-precipitation techniques involves the reduction of iron(III) chloride (0.1 M $FeCl_3 \cdot 6H_2O$ dissolved in 40 mL of 99% ethanol) by 2.5 M of sodium borohydride ($NaBH_4$) solution. The synthesis steps involve the dropwise addition of $NaBH_4$ to $FeCl_3$ ethanol solution with continuous stirring at 200 rpm. The nanoparticles formed were separated by centrifugation and washed with ethanol twice followed by overnight drying in a hot air oven.[18]

4.3. Dead Biomass Preparation. Initial isolation and purification of *Acinetobacter* sp. was performed followed by identification of strain with 16s rRNA sequencing. The regeneration of the *Acinetobacter* sp. was performed by adding 100 μL in 250 mL of nutrient broth (NB) medium (beef extract 0.5 g, yeast extract 1 g, peptone 2.5 g, sodium chloride 2.5 g) followed by resuspension of abovementioned culture of 400 μL in 1000 mL NB medium which was performed to achieve a desired quantity of biomass. Dead biomass was prepared by sterilizing the culture at 121 °C/15 psi and drying it in a vacuum oven overnight at 59 °C.

4.4. Preparation of BNC Bead. Nanocomposite material was prepared by dissolving equal ratio of synthesized Fe_3O_4 and commercial TiO_2 (1:1 ratio) nanoparticles, followed by probe sonication of the abovementioned solution. Preparation of BNC involves the addition of dead biomass (1:2 ratios) into the abovementioned solution. The sample was subjected to sonication in a water bath to get equally dispersed BNC. Prepared BNC was mixed with 25 mL sodium alginate (7%) solution and added dropwise into 100 mL of 2% calcium chloride solution to obtain BNC-immobilized alginate beads.

4.5. Characterization Techniques. The chemically synthesized iron oxide nanoparticles and alginate-encapsulated BNC were characterized by high-resolution scanning electron microscope (FEI Quanta FEG 200) for the analysis of particle size, shape, and morphology with a magnification of 12× to 100 000×. EDX provided elemental composition via back-scattered electron detection system and FT-IR spectroscopy (IR Affinity-1, Shimadzu, Japan) was employed for analyzing the functional groups. The crystalline nature of the BNC bead (before and after interaction) was analyzed by XRD (Bruker Advanced D8, Germany). TOC in the TC-treated samples was measured by the TOC analyzer (Shimadzu) and digital potentiometer (model DP003 PICO, Chennai) was used to analyze the reducing agents present in the TC−BNC interacted solution. Brunauer−Emmett−Teller was used to study the surface porosity of the BNC bead before and after interaction. High-resolution-LC−MS (HR-LC−MS) (1290 infinity UHPLC system, 6550 iFunnel Q-TOFs, Agilent Technologies, USA) was used to detect the degraded products of TC after interaction with nanoparticles.

4.6. Batch Study for TC Removal. TC stock solution (100 mg/L) was prepared and stored in dark at −4 °C well in advance to the work. From the stock solution 40, 20, and 10 mg/L concentration of TC was prepared, and 1, 5, and 10 g of BNC beads was filtered out and interacted with TC for 30 min interval in the UV photoreactor (Heber compact multi-wavelength multilamp photoreactor SW-MW-LW888) under UV-C conditions in borosilicate tubes. The degradation of TC with respect to the control was noted by analyzing the absorbance of the sample at 360 nm. The experiment was carried out in triplicates for statistical purpose. The amount of TC that remained in the test sample can be calculated using the regression equation deduced from the calibration graph, and the percentage of TC removal can be calculated using the equation

$$\text{Removal}\ (\%) = \frac{(A_i - A_f)}{A_i} \times 100 \quad (1)$$

$$\text{Removal capacity}\ (\text{mg/g}) = \frac{A_i - A_f}{m} \times V \quad (2)$$

where A_i and A_f are the initial and final absorbance, m (g) is the mass of the sorbent, and V (L) is the sample volume.

4.7. Kinetic Study. To understand the kinetics of TC removal by the UV-assisted BNC bead, pseudo-first and second-order kinetic models were used. The formula is as follows

$$\ln(q_e - q_t) = \ln q_e - k_1 t \quad (3)$$

where q_t and q_e are used to denote TC adsorbed at time t and at equilibrium t_e; the rate constant of pseudo-first-order model (min^{-1}) was denoted by k_1, which was obtained by plotting $\log(q_e - q_t)$ versus t. However, the formula for the pseudo-second-order kinetics is as follows

$$t/q_t = 1/(k_2 q_e^{\,2}) + t/q_e \quad (4)$$

where k_2 is the pseudo-second-order equilibrium rate constant and which was obtained by plotting t/q_t versus t.

4.8. Residual Toxicity Analysis. The bacterial strain and algal strain were used to study the toxicity of TC and BNC bead-treated TC sample. The bacterial strains were cultured in NB and the algal strains in BG-11 medium. Standard plate count assay was used to analyze cell viability of TC and BNC bead-treated TC interacted cell culture.[8]

■ ASSOCIATED CONTENT

Supporting Information

The Supporting Information is available free of charge on the ACS Publications website at DOI: 10.1021/acsomega.9b02339.

16s rRNA sequencing of the isolated culture; EDX analysis of BNC to find elemental composition; control study to determine TC removal percentage by alginate beads, biosorbent beads, FeO beads, TiO_2 beads under optimization condition; nonphoto-assisted TC removal using the BNC bead under optimized condition to compare with UV-assisted removal (PDF)

■ AUTHOR INFORMATION

Corresponding Author

*E-mail: amit.mookerjea@gmail.com, amitav@vit.ac.in. Phone: +91 416 220 2620.

ORCID

Amitava Mukherjee: 0000-0001-8682-4278

Notes

The authors declare no competing financial interest.

■ ACKNOWLEDGMENTS

We acknowledge Department of Science and Technology-Science and Engineering Research Board (DST-SERB) [EMR/

DOI: 10.1021/acsomega.9b02339
ACS Omega XXXX, XXX, XXX−XXX

2016/004816], Government of India for providing the grant to support this research work.

REFERENCES

(1) Homem, V.; Santos, L. Degradation and Removal Methods of Antibiotics from Aqueous Matrices - A Review. *J. Environ. Manage.* **2011**, *92*, 2304−2347.
(2) Watts, C D; Crathorne, B; Fielding, M; Killops, S D Non-volatile organic compounds in treated waters. *Environ. Health Perspect.* **1982**, *46*, 87−99.
(3) Kang, J.; Liu, H.; Zheng, Y.-M.; Qu, J.; Chen, J. P. Systematic Study of Synergistic and Antagonistic Effects on Adsorption of Tetracycline and Copper onto a Chitosan. *J. Colloid Interface Sci.* **2010**, *344*, 117−125.
(4) Halling-Sørensen, B.; Sengeløv, G.; Tjørnelund, J. Toxicity of Tetracyclines and Tetracycline Degradation Products to Environmentally Relevant Bacteria, Including Selected Tetracycline-Resistant Bacteria. *Arch. Environ. Contam. Toxicol.* **2002**, *42*, 263−271.
(5) Aslan, S.; Yalçin, K.; Hanay, Ö.; Yildiz, B. Removal of Tetracyclines from Aqueous Solution by Nanoscale Cu/Fe Bimetallic Particle. *Desalin. Water Treat.* **2016**, *57*, 14762−14773.
(6) Kosutic, K.; Dolar, D.; Asperger, D.; Kunst, B. Removal of Antibiotics from a Model Wastewater by RO/NF Membranes. *Sep. Purif. Technol.* **2007**, *53*, 244−249.
(7) Koyuncu, I.; Arikan, O. A.; Wiesner, M. R.; Rice, C. Removal of Hormones and Antibiotics by Nanofiltration Membranes. *J. Membr. Sci.* **2008**, *309*, 94−101.
(8) Ravikumar, K. V. G.; Sudakaran, S. V.; Ravichandran, K.; Pulimi, M.; Natarajan, C.; Mukherjee, A. Green Synthesis of NiFe Nano Particles Using Punica Granatum Peel Extract for Tetracycline Removal. *J. Cleaner Prod.* **2019**, *210*, 767−776.
(9) Daghrir, R.; Drogui, P.; Ka, I.; El Khakani, M. A. Photoelectrocatalytic Degradation of Chlortetracycline Using Ti/TiO2 Nanostructured Electrodes Deposited by Means of a Pulsed Laser Deposition Process. *J. Hazard. Mater.* **2012**, *199*−*200*, 15−24.
(10) Safari, G. H.; Hoseini, M.; Seyedsalehi, M.; Kamani, H.; Jaafari, J.; Mahvi, A. H. Photocatalytic Degradation of Tetracycline Using Nanosized Titanium Dioxide in Aqueous Solution. *Int. J. Environ. Sci. Technol.* **2014**, *12*, 603−616.
(11) Olama, N.; Dehghani, M.; Malakootian, M. The Removal of Amoxicillin from Aquatic Solutions Using the TiO2/UV-C Nanophotocatalytic Method Doped with Trivalent Iron. *Appl. Water Sci.* **2018**, *8*, 1−12.
(12) Dimitrakopoulou, D.; Rethemiotaki, I.; Frontistis, Z.; Xekoukoulotakis, N. P.; Venieri, D.; Mantzavinos, D. Degradation, Mineralization and Antibiotic Inactivation of Amoxicillin by UV-A/TiO 2 Photocatalysis. *J. Environ. Manage.* **2012**, *98*, 168−174.
(13) Moreira, N. F. F.; Orge, C. A.; Ribeiro, A. R.; Faria, J. L.; Nunes, O. C.; Pereira, M. F. R.; Silva, A. M. T. Fast Mineralization and Detoxification of Amoxicillin and Diclofenac by Photocatalytic Ozonation and Application to an Urban Wastewater. *Water Res.* **2015**, *87*, 87−96.
(14) Dehghani, M.; Nasseri, S.; Ahmadi, M.; Samaei, M. R.; Anushiravani, A. Removal of Penicillin G from Aqueous Phase by Fe +3 -TiO 2/UV-A Process. *J. Environ. Health Sci. Eng.* **2014**, *12*, 56.
(15) Malakootian, M.; Olama, N.; Malakootian, M.; Nasiri, A. Photocatalytic Degradation of Metronidazole from Aquatic Solution by TiO2-Doped Fe3+nano-Photocatalyst. *Int. J. Environ. Sci. Technol.* **2019**, *16*, 4275−4284.
(16) Tsezos, M.; Bell, J. P. Comparison of the Biosorption and Desorption of Hazardous Organic Pollutants by Live and Dead Biomass. *Water Res.* **1989**, *23*, 561−568.
(17) Aksu, Z.; Tunç, Ö. Application of Biosorption for Penicillin G Removal: Comparison with Activated Carbon. *Process Biochem.* **2005**, *40*, 831−847.
(18) Kandpal, N. D.; Sah, N.; Loshali, R.; Joshi, R.; Prasad, J. Co-Precipitation Method of Synthesis and Characterization of Iron Oxide Nanoparticles. *J. Sci. Ind. Res.* **2014**, *73*, 87−90.
(19) He, D.; Sun, Y.; Xin, L.; Feng, J. Aqueous Tetracycline Degradation by Non-Thermal Plasma Combined with Nano-TiO2. *Chem. Eng. J.* **2014**, *258*, 18−25.
(20) Huang, B.; Liu, Y.; Li, B.; Liu, S.; Zeng, G.; Zeng, Z.; Wang, X.; Ning, Q.; Zheng, B.; Yang, C. Effect of Cu(II) Ions on the Enhancement of Tetracycline Adsorption by Fe3O4@SiO2-Chitosan/Graphene Oxide Nanocomposite. *Carbohydr. Polym.* **2017**, *157*, 576−585.
(21) Nalbandian, L.; Patrikiadou, E.; Zaspalis, V.; Patrikidou, A.; Hatzidaki, E.; Papandreou, C. N. Magnetic Nanoparticles in Medical Diagnostic Applications: Synthesis, Characterization and Proteins Conjugation. *Curr. Nanosci.* **2016**, *12*, 455−468.
(22) Ho, Y. S.; Mckay, G. Pseudo-Second Order Model for Sorption.Pdf. *Process Biochem.* **1999**, *34*, 451−465.
(23) Ravikumar, K. V. G.; Singh, A. S.; Sikarwar, D.; Gopal, G.; Das, B.; Mrudula, P.; Natarajan, C.; Mukherjee, A. Enhanced Tetracycline Removal by In-Situ NiFe Nanoparticles Coated Sand in Column Reactor. *J. Environ. Manage.* **2019**, *236*, 93−99.
(24) Chou, C.-S.; Chen, C.-Y.; Lin, S.-H.; Lu, W.-H.; Wu, P. Preparation of TiO2</Inf>/Bamboo-Charcoal-Powder Composite Particles and Their Applications in Dye-Sensitized Solar Cells. *Adv. Powder Technol.* **2015**, *26*, 711−717.
(25) Dalmázio, I.; Almeida, M. O.; Augusti, R.; Alves, T. M. A. Monitoring the Degradation of Tetracycline by Ozone in Aqueous Medium Via Atmospheric Pressure Ionization Mass Spectrometry. *J. Am. Soc. Mass Spectrom.* **2007**, *18*, 679−687.
(26) Tabrizian, P.; Ma, W.; Bakr, A.; Rahaman, M. S. PH-Sensitive and Magnetically Separable Fe/Cu Bimetallic Nanoparticles Supported by Graphene Oxide (GO) for High-Efficiency Removal of Tetracyclines. *J. Colloid Interface Sci.* **2019**, *534*, 549−562.
(27) He, L.; Dong, Y.; Zheng, Y.; Jia, Q.; Shan, S.; Zhang, Y. A Novel Magnetic MIL-101(Fe)/TiO 2 Composite for Photo Degradation of Tetracycline under Solar Light. *J. Hazard. Mater.* **2019**, *361*, 85−94.
(28) Reyes, C.; Fernández, J.; Freer, J.; Mondaca, M. A.; Zaror, C.; Malato, S.; Mansilla, H. D. Degradation and Inactivation of Tetracycline by TiO 2 Photocatalysis. *J. Photochem. Photobiol., A* **2006**, *184*, 141−146.
(29) Qu, L.-L.; Wang, N.; Li, Y.-Y.; Bao, D.-D.; Yang, G.-H.; Li, H.-T. Novel Titanium Dioxide−Graphene−Activated Carbon Ternary Nanocomposites with Enhanced Photocatalytic Performance in Rhodamine B and Tetracycline Hydrochloride Degradation. *J. Mater. Sci.* **2017**, *52*, 8311.
(30) Shi, Y.; Yang, Z.; Wang, B.; An, H.; Chen, Z.; Cui, H. Adsorption and Photocatalytic Degradation of Tetracycline Hydrochloride Using a Palygorskite-Supported Cu2O−TiO2 Composite. *Appl. Clay Sci.* **2016**, *119*, 311−320.

DOI: 10.1021/acsomega.9b02339
ACS Omega XXXX, XXX, XXX−XXX